Dynamic Climbing Ropes: A Numerical Analysis of Rope Properties

Close to 200 climbing ropes currently on the market were assessed using a numerical model. Commonly available values provided by the rope manufacturers were evaluated, including peak (impact) force, dynamic elongation and static elongation. The numerical simulation used a three-parameter viscoelastic rope-model to calculate the dynamic and static loads in a range of climbing fall scenarios. By applying this model, the behaviour of different ropes was simulated and key performance characteristics identified. The results showed that ropes with lower peak forces and higher dynamic elongations performed much better in all scenarios, leading to lower maximum accelerations, higher energy absorption, less jerk and lower forces on all components of the safety chain during fall arrest. This greatly reduces the risk of injury in climbing and mountaineering falls. The influence of the static elongation was minor, however. Even though all assessed ropes met the requirements of the relevant European Standard, it was found that only about one third had the desired combination of low peak force and high dynamic elongation.

Keywords: *mountaineering, numerical simulation, rock climbing, rope properties, single dynamic rope*

Introduction

Early mountaineering ropes made of natural fibres (typically hemp) could only withstand small loads and had very limited energy absorbing capability. These so-called hawser laid ropes were made of three intertwined strands, where each strand consisted of yarns and these in turn of fibres twisted together. Tests done by the English Alpine Club in 1864 showed that such ropes could only sustain a fall of 10 feet (around 3 m) for a weight of 168 lb (75 kg) (Smith, 1998). This meant a lead fall would most certainly be fatal, hence the old adage 'the leader must not fall'.

Since the 1950's mountaineering and climbing ropes have been manufactured from polyamide (nylon) in a kernmantel construction, where a sheath (mantle) is tightly braided about a core (kern) (Andrew, 2006). The yarns used for both core and sheath are continuous filaments. The raw yarn is twisted into a twine, which in turn is twisted into strands, which are then intertwined to form the final rope. Along with the tensile strength and modulus of elasticity of the raw material the number of twists per meter determine ultimate rope strength and stretch (Karrer, 2002). The energy absorbing qualities of the rope are mainly determined by the core, while the mantle provides abrasion resistance (Beal, 2002).

These modern ropes can easily withstand significant lead falls while minimising the peak force (or impact force, Andrew, 2006) acting on the climber, the belayer and all parts of the safety chain. This development gave birth to sports climbing and allowed mountaineers to push the limits. Nowadays, rope breaks are very rare and typically only occur if the rope is running over sharp edges or if it previously had been chemically or mechanically damaged (Schubert, 2000).

According to the European Standard EN 892:2012 (EN 892, 2012), dynamic mountaineering ropes are defined as ropes capable of arresting the free fall of a person engaged in mountaineering or climbing with a limited peak force. They have to fulfil a great number of requirements (Blackford, 2003), which can be divided into the four categories: *safety, human comfort, durability and handling*.

In the safety category, it is not only high strength and energy absorption ability that are required, but also minimum impact on the safety chain, high sharp edge strength, low static elongation as well as invariability of mechanical properties under environmental influences (water, temperature). For human comfort, it is desirable to have minimal peak force and jerk during fall arrest. As far as durability is concerned, attributes like slow environmental aging, high resistance to UV radiation and wear, little loss of performance characteristics and ability to withstand a large number of falls are paramount. Lastly, to give a rope a good handling it should have low weight, good ‘feel’, high flexibility and a low tangling susceptibility.

Some of these requirements are contradictory, such as high strength and low weight, while others come down to a pure personal preference. Also, consumers will be driven by aspects such as aesthetics, brand reputation and costs.

While it is obvious that certain parameters are paramount to climbing safety (e.g. tensile strength, edge resistance), the impact of some of the others on the safety chain is less clear. This paper examines the characteristics from the safety and human comfort categories of close to *200 dynamic single ropes* currently on the market. The key parameters are identified and evaluated with numerical methods and their implications on climbing safety and rope selection are discussed.

General Safety Requirements of Dynamic Single Climbing Ropes

Dynamic single mountaineering or climbing ropes are ‘equipment for protection against falls from a height’ and are in the scope of the European Directive 89/686/EEC, Personal Protective Equipment (PPE). Single ropes are capable of being used singly as a link in the safety chain to arrest a leader’s fall (European Directive 89/686/EEC, 2013). They are category III or ‘complex design’ PPE (PPE Guidelines, 2010). The directive defines amongst other things the *basic health and safety requirements and the certification procedures*.

All basic safety requirements are met by applying and meeting the requirements of the harmonized European Standard EN 892:2012 (EN 892, 2012), mountaineering equipment – dynamic mountaineering ropes – safety requirements and test methods. This applies only for ropes in kernmantel construction. A manufacturer that has followed the complete certification procedure is allowed to CE mark the rope and put it on the market. The requirements as per EN 892:2012 include a maximum peak force of 12 kN and a maximum dynamic elongation of 40 % during the first drop, a static elongation of no more than 10 % and the ability to withstand at least 5 consecutive drop tests without breaking.

Peak force, dynamic elongation and number of drops are determined with a standard drop test (see Figure 1), where a mass of 80 kg drops 4.8 m, held by a rope length of 2.8 m. The *peak force* is the maximum force applied by the rope on a load cell attached to the falling mass. The *dynamic elongation* is the peak rope extension relative to the nominal length of 2.8 m. The *number of drops* is determined by performing repetitive drop tests until rope rupture. Lastly, the *static elongation* is the change in length one metre of rope undergoes when weighted with 80 kg.

Figure 1. *Fall Geometry for Standard Drop Test According To EN 892:2012: (A) Before And (B) After the Drop*

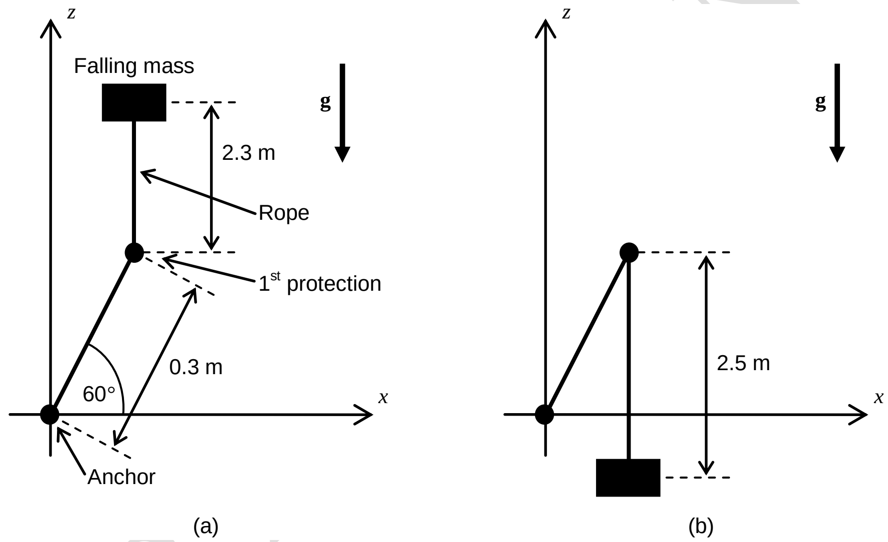

The International Mountaineering and Climbing Federation, UIAA (Union Internationale des Association d'Alpinisme) is an independent organisation founded 1932 with the goal to "study and find solutions of all problems regarding mountaineering" (http://www.theuiaa.org). The UIAA was the first organisation globally to create standards for mountaineering and climbing equipment (UIAA, 2013). Many of these requirements have been integrated into the European Standards by the European Committee for Standardisation CEN (Comité Européenne de Normalisation). Today, the UIAA standards are based on the EN standards in order to avoid the confusion of having multiple standards. The UIAA standards sometimes apply higher and/or additional requirements to the EN standards.

The standard UIAA 101-6.0 (UIAA 101-6.0, 2014), mountaineering equipment – dynamic ropes, defines *additional* requirements for dynamic mountaineering ropes. Only ropes that comply *both* with the standards EN 892 and UIAA 101 may carry the UIAA Safety Label. Additional requirements of UIAA 101-6.0 compared to EN 892:2012 include the ability to withstand 10, rather than 5 drop tests for multidrop ropes and requirements regarding maximum weight increase due to water absorption. Furthermore, the energy absorbed before rupture per unit length needs to be determined with an additional drop test using a larger mass of 100 kg and having the rope run over a sharp edge orifice plate with a radius of 0.75 mm, meaning it is a measure of notch sensitivity. 1.6 kJm^{-1} is considered a low value, 1.9 kJm^{-1} high.

Methods

Author (2014) presented a program to numerically model rock climbing falls. It correctly predicts the forces acting on climber, belayer, rope and all other elements of the safety chain in a wide range of scenarios. This program considers real rope and belay device characteristics, rope friction, energy absorbed by the climber and air drag. It is based on the integration of the basic equation of motion for both the climber and the belayer. It employs a three-parameter, viscoelastic rope model (also known as standard linear solid or Zener model) to describe the mechanical properties of the dynamic climbing rope as proposed by Pavier (1998). Figure 2 shows the model under the load of a rope force F_{Rope}. A spring K_{R2} is in series with an in-parallel combination of another spring K_{R1} and a dashpot D_R.

Figure 2. *Three-Parameter Viscoelastic Rope Model*

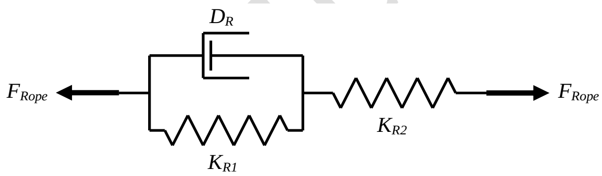

This rope model was found to best simulate the behaviour of the rope under dynamic and static loading conditions. The rope parameters are calibrated using actual real rope values provided by the rope manufacturers, including peak force, dynamic and static elongation.

To be able to simulate different fall situations with various rope lengths, rope parameters based on a rope length of one meter are used ($K_{R1Meter}$, $K_{R2Meter}$ and D_{RMeter}), obtained by dividing the rope parameters by the total paid out rope length L_{Tot}, giving

$$K_{R1} = \frac{K_{R1Meter}}{L_{Tot}}, \quad K_{R2} = \frac{K_{R2Meter}}{L_{Tot}} \quad \text{and} \quad D_R = \frac{D_{RMeter}}{L_{Tot}} \qquad (1).$$

Author's program correctly calculates the forces and accelerations encountered in different fall scenarios. This allows *comparing the rope behaviour in real world situations* (as opposed to merely a standard drop test) based on rope values available from the manufacturers.

Materials

Rope Values

A large number of dynamic single climbing ropes are available on the market, with diameters ranging from 9 to 12 mm. A non-exhaustive selection of 175 ropes from 25 manufacturers has been chosen for this analysis, representing the vast majority of rope models currently in use. Table 1 shows all ropes manufacturers and number of ropes considered for the evaluation.

Table 1. *25 Rope Manufacturers Used for Evaluation*

Austrialpin: 2	Beal: 14	Blacksafe: 2	Blue Water: 8
CAMP: 6	Consolidated Cordage: 3	Cousin: 7	CT: 1
Edelrid: 14	Edelweiss: 8	Gilmonte: 3	Kaya: 9
Mammut: 13	Metolius: 4	Millet: 8	New England: 11
Petzl: 5	PMI: 7	Ridgegear: 1	Roca: 12
Singing Rock: 7	Skylotec: 4	Sterling: 10	Tendon: 12
Trango: 4			

Some rope display only partial information on their product information sheets so they could not be used for the evaluation (Anpen, DMM, Marlow and Salewa).

This evaluation only includes single ropes that comply with the European Standard EN 892. Five rope values given by the manufacturers (e.g. found on hand tags) were compared with statistical methods and evaluated in a numerical simulation. The method is described in detail in Spoerri (2014).

Peak force PF, dynamic elongation DE, static elongation SE, rope diameter D_R and rope mass per meter m_R were utilised and normalized to PF_N, DE_N, SE_N, D_{RN}, m_{RN} using the arithmetic mean of all evaluated ropes PF_{Mean}, DE_{Mean}, SE_{Mean}, DR_{Mean}, m_{RMean}, giving

$$PF_N = \frac{PF}{PF_{Mean}} \quad (2).$$

Table 2 lists the obtained mean rope values.

Table 2. *Arithmetic Mean Values of all Analysed 175 Ropes*

Name	*Variable*	*Unit*	*Value*
Peak force mean value	PF_{Mean}	kN	8.4
Dynamic elongation mean value	DE_{Mean}	%	33.3
Static elongation mean value	SE_{Mean}	%	7.7
Rope diameter mean value	DR_{Mean}	mm	9.9
Rope mass per meter mean value	m_{RMean}	kgm^{-1}	0.064

Table 3 shows the standard deviation as well as the 1st and 2nd quartile of the analysed rope values. It can be seen that for some parameters like peak force, the spread is fairly narrow, while static elongation and rope mass and diameter show greater variability between the different ropes.

Table 3. *Statistic Values of Rope Normalized Rope Values*

Normalized rope value	*Standard deviation*	*1st quartile (25 %)*	*2nd quartile (75 %)*
Peak force	0.6 kN	8.0 kN	8.8 kN
Dynamic elongation	2.5 %	31.7 %	35.0 %
Static elongation	1.4 %	6.5 %	9.0 %
Rope diameter	0.6 mm	9.5 mm	10.2 mm
Rope mass per meter	0.007 kgm^{-1}	0.059 kgm^{-1}	0.068 kgm^{-1}

Figure 3a plots dynamic elongation versus peak force. It is evident that all values are located in a band going from the second to the fourth quadrant. There is no correlation between the dynamic elongation and the rope diameter (Figure 3b).

Figure 3. *Normalized Rope Values: (a) Dynamic Elongation vs. Peak Force, (b) Dynamic Elongation vs. Rope Diameter*

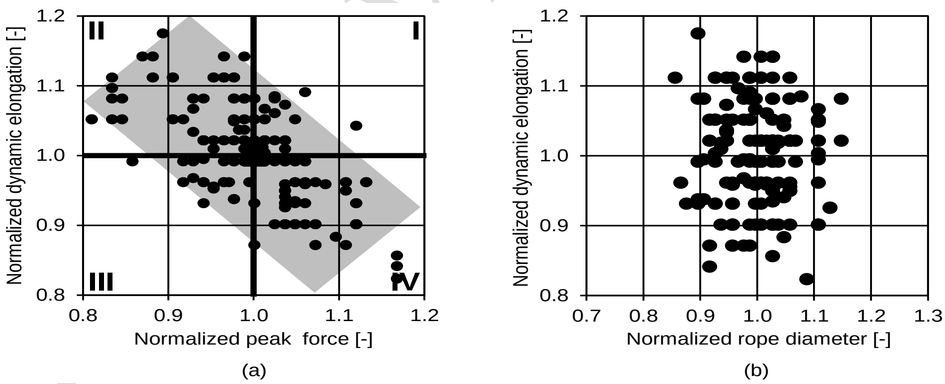

Table 4 summarizes the distribution of the ropes within the four quadrants in Figure 3a. The majority of the ropes are located in the second and the fourth quadrant (71.4 %), fewer ropes are in the first and third quadrant (28.6 %).

Table 4. *Distribution of the 175 Normalized Ropes with Respect to Impact Force and Dynamic Elongation*

Quadrant	*Number of ropes*	*Percentage*
Quadrant I	29	16.6 %
Quadrant II	**59**	**33.7 %**
Quadrant III	21	12.0 %
Quadrant IV	**66**	**37.7 %**

In contrast, the static elongation does not show any correlation with either the peak force (Figure 4a) or the rope diameter (Figure 4b).

Figure 4. *Normalized Rope Values: (a) Static Elongation vs. Peak Force, (b) Static Elongation vs. Rope Diameter*

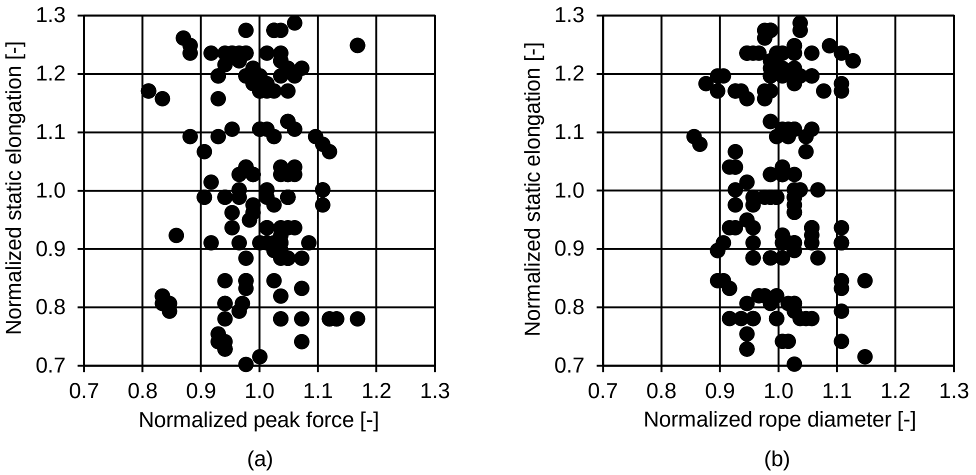

Rope mass and rope diameter are clearly correlated, however. Figure 5 shows the distribution of the ropes and the fitted linear and the polynomial second order lines, obtained using the least squares method. The rope mass can be calculated with good accuracy (R^2 = 0.931) using

$$m_R = 11.491 D_R - 0.050 \qquad (3).$$

The difference between he first and the second order function is less than 0.9 % for rope diameters between 9 and 11 mm. The linear relationship between rope mass per length and diameter shows that the rope density is very similar for all manufacturers. While unsurprising, this could not be taken for granted since the ropes might have slightly different constructions within the same basic design.

Figure 5. *Normalized Rope Mass vs. Normalized Rope Diameter*

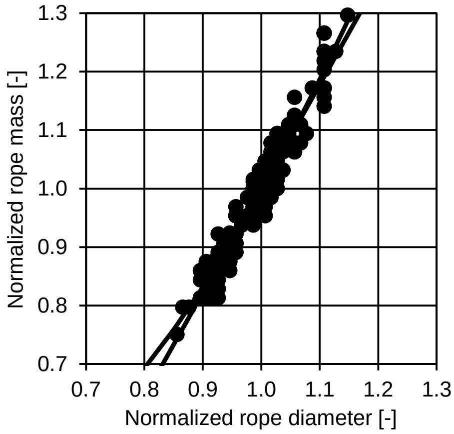

Figure 6a depicts the distribution of peak force, dynamic elongation and rope diameter. There is a clear similarity with all three parameters showing close to normal distribution, indicating that these might be linked. The static elongation (see Figure 6b) on the other hand exhibits a more random distribution. It is not surprising that there is a significant spread in values for the assessed ropes. Even though they are all made from polyamide, different braiding patterns, core/mantle ratios or fibre coating and pre-treatments easily account for the differences.

Figure 6. *Distribution of Normalized Rope Values: (a) Peak Force, Dynamic Elongation and Rope Diameter, (b) Static Elongation*

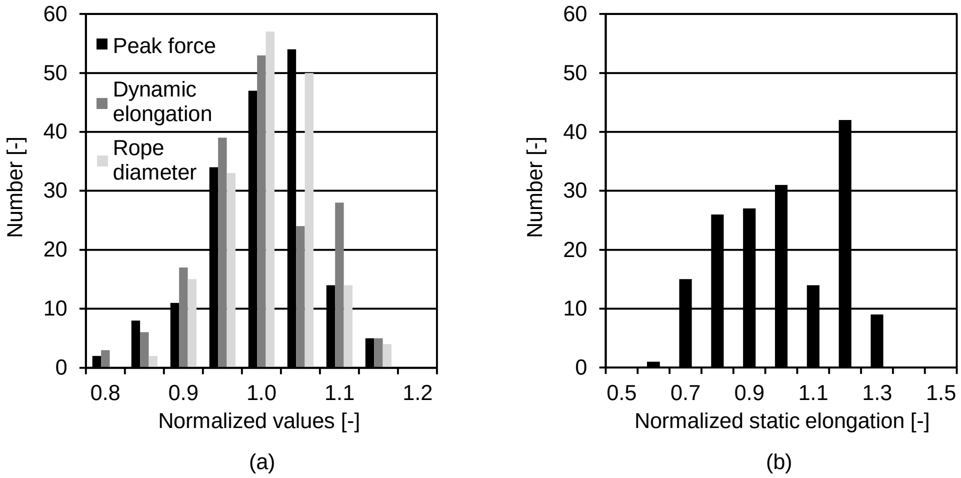

Definition of Test Ropes

In order to numerically analyse the rope properties with respect to different rope values, a ‘basic test rope’ was defined using the calculated averages from the 175 ropes included in this study (see Tab. 2); the values are listed in Table 5. Note that the subscripts ‘Test’ and ‘Mean’ refer to the same values.

Table 5. *'Basic Test Rope' Values*

Name	*Variable*	*Unit*	*Value*
Peak force	PF_{Test}	kN	8.4
Dynamic elongation	DE_{Test}	%	33.3
Static elongation	SE_{Test}	%	7.7

These values were fed into the simulation and varied by ±1 kN for the peak force (in steps of 0.5 kN), ±4 % for the dynamic elongation (in steps of 2 %) and ±2 % for the static elongation (in steps of 1 %). Figure 7a shows the coverage of the test ropes values in comparison to the real rope values with respect to peak force and dynamic elongation; Figure 7b the coverage with respect to static elongation. These figures demonstrate that the vast majority of commercially available ropes are covered by this analysis.

Figure 7. *Coverage of Normalized Test Rope Values for Simulation: (a) Dynamic Elongation vs. Peak Force, (b) Static Elongation vs. Peak Force*

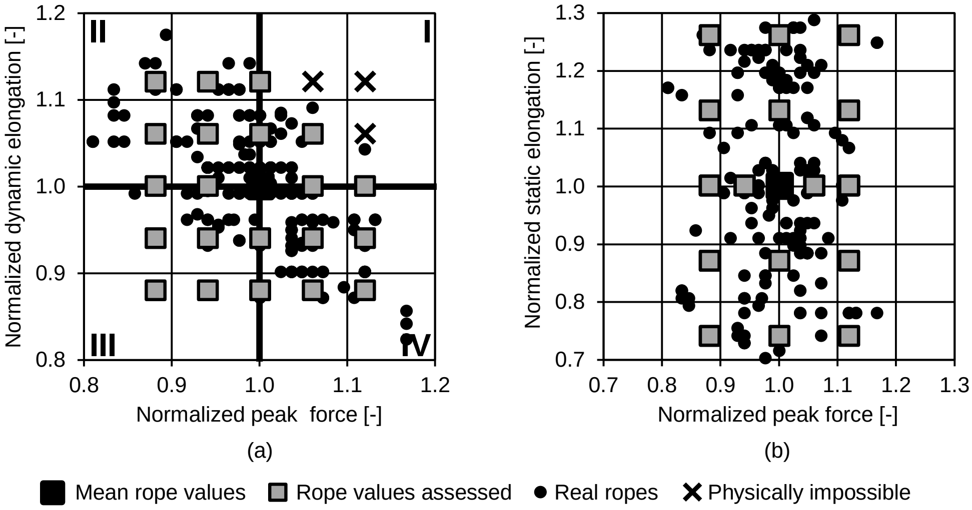

Table 6 summarizes the calibrated rope parameters for the 'basic test rope'. There is a calibration mode in the simulation (Author, 2014), where for any given real rope values *(PF*, *DE* and *SE*), the three rope parameters ($K_{R1Meter}$, $K_{R2Meter}$ and D_{RMeter}) can be calibrated. Within the calibration mode, the same setup as given in the Standard (EN 892, 2012) is used and the simulation results compared with the real rope values. If the deviation of each of the simulated to the measured rope values is less than a specified threshold value (e.g. 0.01 %) the calibration is stopped otherwise the program runs another iteration with altered rope parameters. Analysis has shown that the same rope parameters are obtained regardless of the initial parameters fed into the simulation.

The geometry used for the simulation is shown in Figure 1. The program considers friction at the 1st protection (orifice), friction in the guide of the falling mass, air drag and the knot used to tie the rope to the falling mass. For the 'basic test rope', the energy absorbed by the rope is 92.5 %, while the contributions of friction at the orifice, friction in the guide, air drag and knot are 5.7, 0.4, 0.1 and 1.3 %, respectively. The total rope length according to (1) is 2.8 m. The program does not find reasonable solutions for the rope values marked with a ‘cross’ (designated physically impossible) in Figure 7a, as the values for the rope parameter D_{RMeter} go to physically meaningless high values. They are thus not included in this analysis.

Table 6. *‘Basic Test Rope’ Parameters*

Name	*Variable*	*Unit*	*Value*
Rope damping constant per meter	D_{RMeter}	Ns	9902
Rope spring constant 1 per meter	$K_{R1Meter}$	N	13751
Rope spring constant 2 per meter	$K_{R2Meter}$	N	31317

Results

Calculated Rope Parameters

The calculated rope parameters are normalized using parameters of the ‘basic test rope’. Figure 8 shows the rope spring constant 1 and 2 for different peak forces and a constant static elongation.

Figure 8. *Normalized Rope Parameters vs. Normalized Peak Force: (a) Spring Constant 1, (b) Spring Constant 2. The Normalization is 9-= βββ from Table 5 or Table 6*

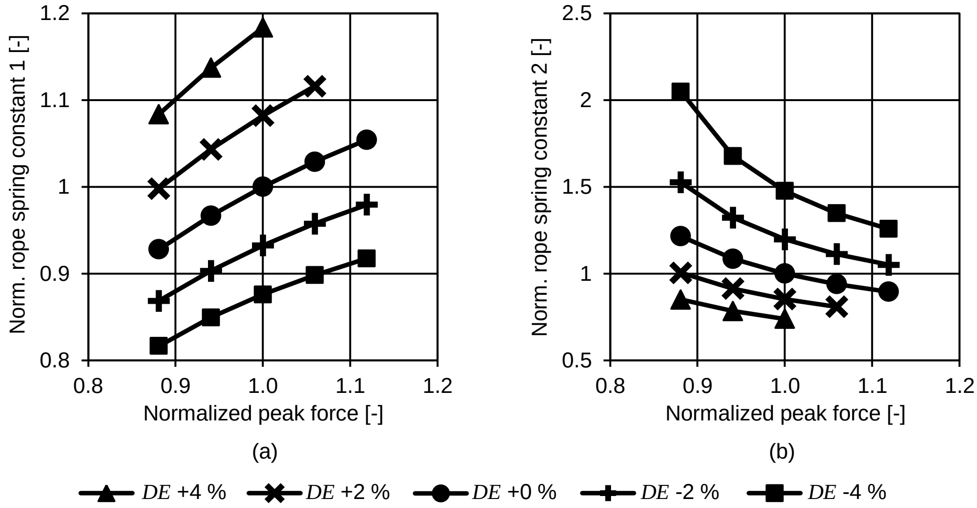

Figure 9 shows the rope damping constant for different peak forces and a constant static elongation. The curve for the dynamic elongation of the ‘basic test rope ‘(*DE* +0 %) shows a very steep slope for rising normalized peak forces. This behaviour is even more distinct for higher dynamic elongations (*DE* +2 % and *DE* +4 %). This is where the values for the rope parameter D_{RMeter} go to physically meaningless high values as mentioned before.

Figure 9. *Normalized Rope Damping Constant vs. normalized peak force. The normalization is done using values from Table 5 or Table 6*

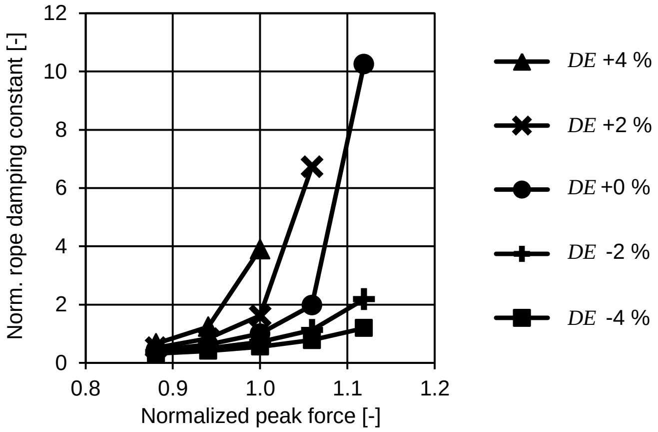

The ratio of K_{R1} to K_{R2} changes when varying static elongation (Figure 10a), while the damping constant D_R (Figure 10b) does not change significantly; the data points overlap for all levels of *SE*. The high values of D_R presented in Figure 10b (around 10) reflect the behaviour of the rope damping constant with increasing peak forces as shown in Figure 9.

Figure 10. *Normalized Rope Parameters: (a) Spring Constant 1 vs. Spring Constant 2, (b) Damping Constant vs. Spring Constant 2. The Normalization is Done Using Values from Table 6*

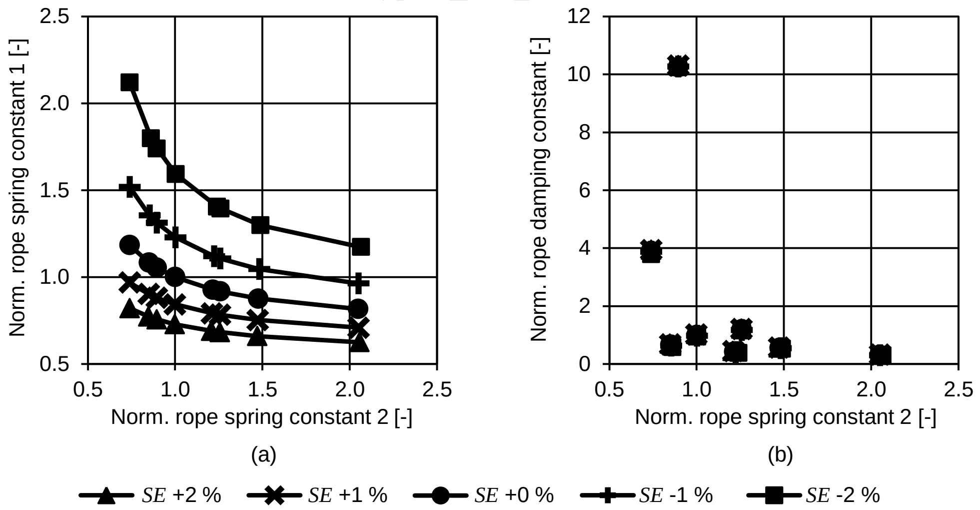

Characteristic Rope Properties for Evaluation

The maximum energy absorption per meter, the maximum acceleration and the maximum jerk have been selected to numerically evaluate and discuss rope performance.

Maximum Energy Absorption Per Meter

As described earlier, the standard UIAA 101-6.0 (UIAA 101-6.0, 2014) describes an additional value, the energy absorbed before rupture per unit rope length. It too is obtained by a drop test, but this time the force $F(t)$ is recorded over time, and the mass displacement $s(t)$ calculated by integrating the equation of motion for the frictionless falling mass, giving

$$s(t) = \frac{1}{M} \int_{t_{start}}^{t} \int_{t_{start}}^{t} \left[M\, g - F(t) \right] dt\, dt \quad (4).$$

where t_{start} is the starting time where the rope is first stretched and t_{rupt} is the time where the rope breaks. The energy absorbed before rupture E_{rupt} is then obtained by integrating the force $F(s)$ along the path ds, yielding

$$E_{rupt} = \int_{s_{tens}}^{s_{rupt}} F(s)\, ds \quad (5),$$

with s_{tens} the starting position where the rope is first stretched $s_{tens} = s(t_{tens})$ and s_{rupt} the position where the rope breaks $s_{rupt} = s(t_{rupt})$.

The final energy absorbed per unit rope length E_u is calculated by dividing the energy absorbed before rupture E_{rupt} by the reference rope length L_{ref}, which yields

$$E_u = \frac{E_{rupt}}{L_{ref}} \quad (6).$$

To evaluate the energy absorption qualities of the test ropes, the standard drop situation is simulated using a falling mass of 100 kg and the energy according to (6) is calculated assuming a rope rupture at 8.4 kN; the peak force value of the ‘basic test rope’ (see Tab. 5). This assumption has been made since no energy indications are yet available from rope manufacturers. The notch sensitivity of the ropes cannot be numerically simulated and therefore is not taken into account.

Figure 11 shows the energy absorption per unit for different peak forces and dynamic elongations. Quadrant II ropes (see Figure 7a, $PF_N < 1$, $DE_N > 1$) clearly have a much higher energy absorption than quadrant IV ropes ($PF_N > 1$, $DE_N < 1$), with the highest value (1.35) being almost twice the lowest (0.76). For the same dynamic elongation, the energy absorption per unit is decreasing with increasing peak force; stiffer ropes have a lower energy absorption capability.

Figure 11. *Normalized Energy Absorption per Unit of Rope vs. Normalized Peak Force*

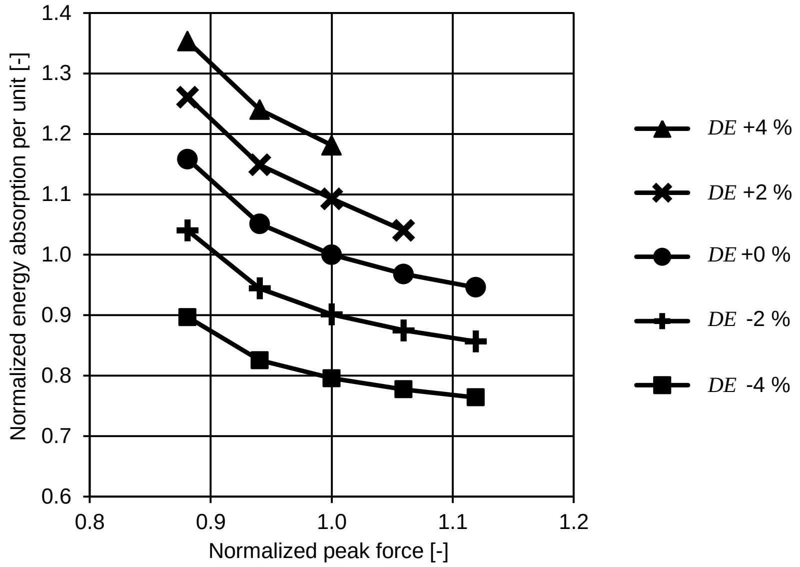

On the other hand, the influence of the static elongation is minor with a variation in absorbed energy of less than 4 % (not plotted).

<u>*Maximum acceleration*</u>

The maximum acceleration a_{Max} experienced during a fall is solely a function of the maximum rope force F_{Max} and the mass of the climber M_C. For a standard drop situation it can be calculated applying Newton's law in the direction of the acceleration of gravity g, resulting in

$$a_{Max} = \frac{F_{Max}}{M_C} \qquad (7).$$

Figure 12a shows the maximum acceleration for different peak forces obtained using equation 7 and the results from the peak force simulations. The acceleration is given as a multiple of g (9.81 ms^{-2}). Figure 12b shows the time curve of the acceleration for the standard drop using the parameters of the 'basic test rope'. The 'start' acceleration is -1 g (i.e. downward gravity), the maximum value 9.7 g (upward 'pull' by the rope), giving a maximum acceleration a_{Max} of 10.7 g using a maximum rope force of F_{Max} of 8.4 kN and a falling mass M_C of 80 kg in Equation (7).

Figure 12. *Acceleration (with Characteristic Points as Mentioned in text): (a) Maximum Acceleration vs. Peak Force, (b) Acceleration for the 'Basic Test Rope' Over Time*

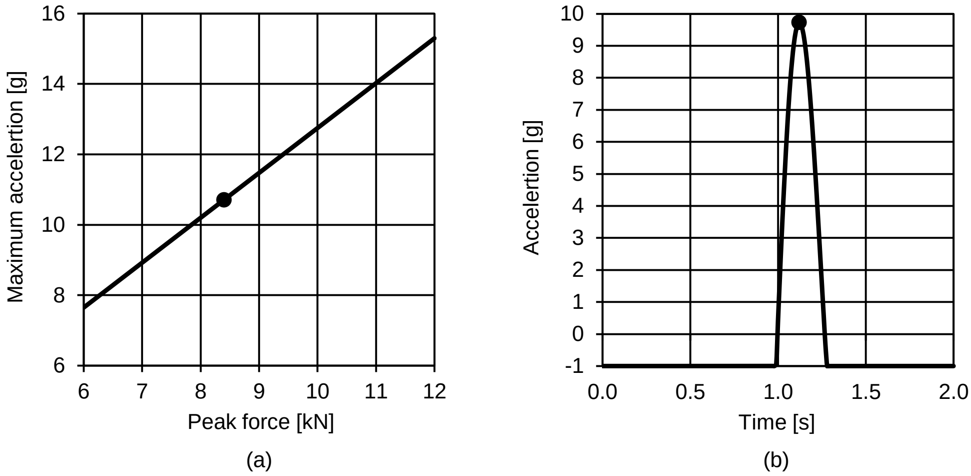

The impact of high accelerations on the human body depends on magnitude, duration and direction (i.e. transverse, lateral or vertical) (Voshell, 2004). Large accelerations in vertical direction (head to toe) can lead to G-induced loss of consciousness (G-LOC) (Burton & Whinnery, 1985). This is a well-known danger for fighter pilots and astronauts. While the acceleration of 10.7 g in a standard drop is high enough for G-LOC (which starts at around 5 g), the duration of 0.3 s (see Figure 12b) is too short, and the average value over the whole deceleration is only around 6.9 g. Unconsciousness does not occur until after some 5 s of constant accelerations (Voshell, 2004). An acceleration of 10.7 g is also not expected to lead to significant trauma to the brain; the injury threshold in racing car accidents is closer to 50 g (Weaver, Sloan, Brizendine & Bock, 2006).

The consequences of an acceleration of 10.7 g on the musculoskeletal system are less clear. While 12 g is considered survivable, NASA/AGARD research nevertheless showed a 5 % injury risk at that level (Crawford, 2003).

Another factor to consider is the fall height. In sports climbing, the highest loads will occur in factor two falls, where the fall height is equal to twice the used rope length. In that scenario, the maximum acceleration is actually higher for shorter falls, as show in Figure 13. While this may seem counterintuitive, it can be explained by the fact that there is less rope length available for energy absorption and the fall will feel 'harder'. On the other hand, since the fall is shorter the duration is also shorter (see right-hand axis in Figure 13). It needs to be mentioned that for very short falls the deformation of the body come into effect as well, leading to somewhat lower accelerations in a real life scenario. Regardless of fall height, there is no danger for G-LOC, but injuries such as strains, sprains and fractures are possible in such a situation.

Figure 13. *Maximum Acceleration and Time for Fall Factor two fall (M_C = 80 kg) for Different Fall Heights*

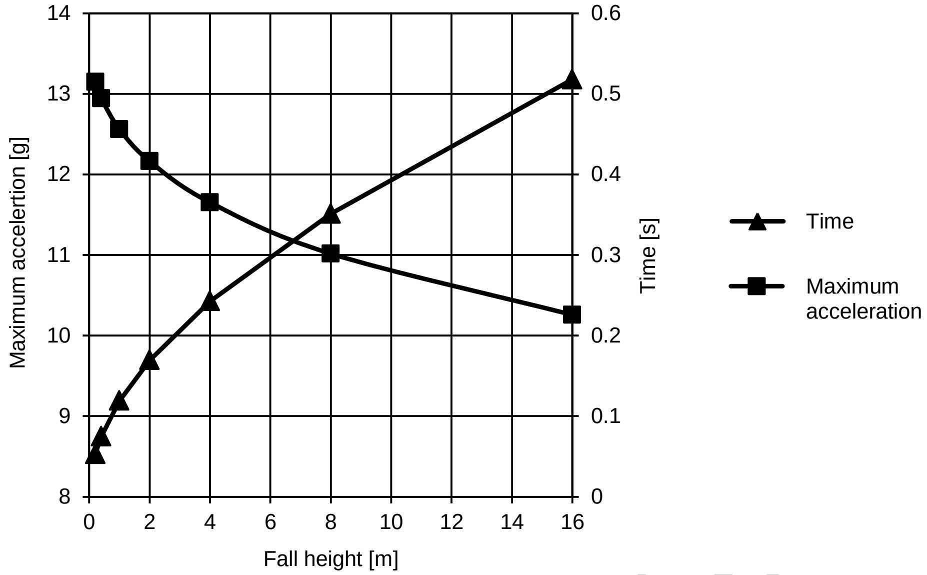

Maximum Jerk

The jerk j describes the rate of change of the acceleration $a(t)$ over time, i.e. the first derivative of the acceleration as per

$$j = \frac{da(t)}{dt} \quad (8).$$

To evaluate the jerk behaviour of the ropes, the standard drop situation is simulated and the maximum jerk recorded. Figure 14 shows the maximum jerk for different peak forces and dynamic elongations. Ropes with higher dynamic elongations show a significantly lower maximum jerk; the values range from roughly 0.75 to 2; a difference of well over 150 %.

Figure 14. *Normalized Maximum Jerk vs. Normalized Peak Force*

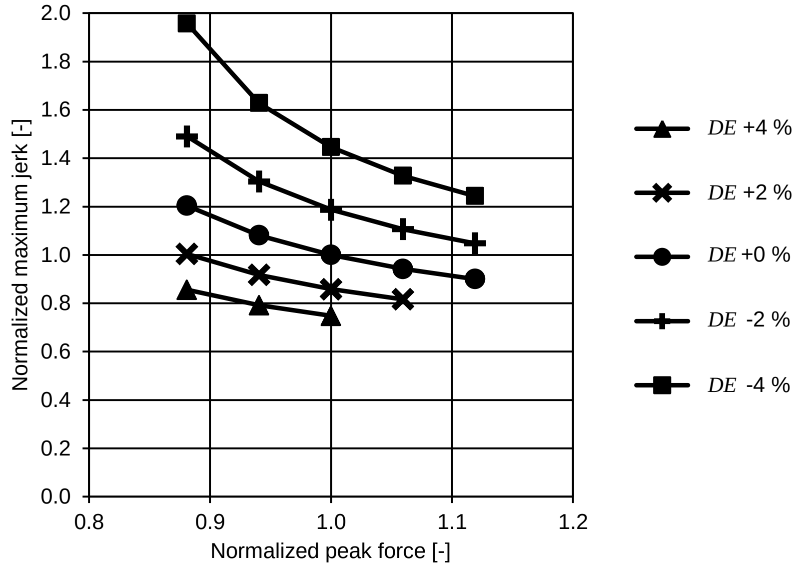

The effect of dynamic elongation on jerk is also shown in Figure 15, depicting the time curve of the jerk for the standard drop using the parameters of the 'basic test rope' (Figure 15a) and a rope with increased dynamic elongation of +4 % (Figure 15b). The maximum jerk decreases by 33.7 %.

Figure 15. *Jerk Time Curve: (a) Parameters 'Basic Test Rope', (b) Parameters 'Basic Test Rope' with Increased Dynamic Elongation (+ 4 %)*

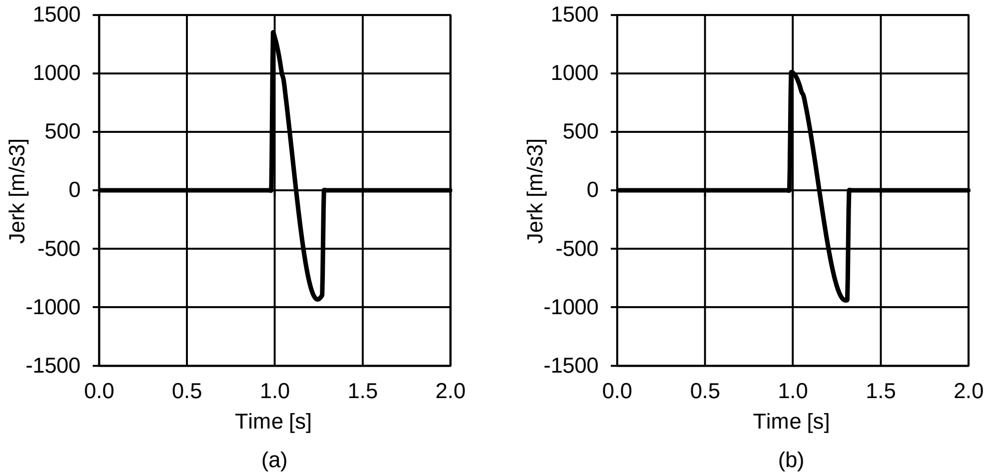

The influence of the static elongation on the maximum jerk is minor, however. A difference of less than 2 % was calculated for the ropes with maximum and minimum static elongation.

In terms of climbing safety, the maximum jerk is much more relevant than the maximum acceleration. It can cause serious injury (Reali & Stefanini, 1996) to the musculoskeletal system if it is too high. This is due to the fact that climbers typically utilise harnesses tied around the waist, where the anchor point sits below the centre of gravity of the human body. This means the jerk experienced in a large fall can lead to severe overstraining of the spine. In addition, it can cause the climber to rotate backwards and impact the rock face with the back of the head. If a chest harness is used, on the other hand, compression injuries to the thorax can occur (Lutz & Mair, 2002).

What Is The 'Ideal' Rope?

The analyses and discussions above clearly show that a low peak force and a high dynamic elongation are preferable. This leads to a higher energy absorption capability, lower maximum acceleration as well as lower maximum jerk, thus greatly reducing the injury risk. A low peak force is also desirable, since it helps limit the load on all protection points within the safety chain (Bennet, 2000). Some of these can have breaking strength of less than 8 kN, particularly karabiners loaded in a non-ideal manner (Schambron & Uggowitzer, 2009) and passive protection such as nuts and camming devices. For all these reasons, quadrant II ropes in Figure 7a are clearly the ropes of choice from a safety point of view. This covers 59 of the analysed ropes, or just over one third (see Tab. 4).

However, there is an upper limit to the dynamic elongation. If that value gets too high, the actual fall height is greatly increased, meaning the climber might hit the ground or a ledge before the fall has been fully arrested by the rope. In addition, the 'bungee effect' associated with very flexible ropes could cause the climber to impact the rock face upon rebound.

As shown in Figure 16, quadrant II ropes are not associated with a particular diameter or static elongation. This is also evident in the distribution of these parameters among the quadrant II ropes in Figure 17; the pattern is similar to the distribution of all evaluated ropes in Figure 6.

Figure 16. *Normalized Values for Quadrant II Ropes: (a) Rope Diameter, (b) Static Elongation*

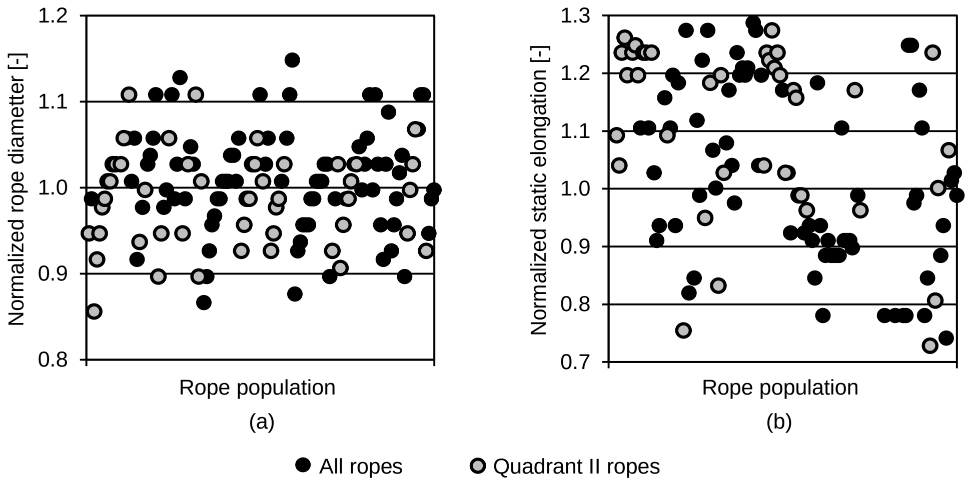

Figure 17. *Distribution of Normalized Quadrant II Rope Values: (a) Rope Diameter, (b) Static Elongation*

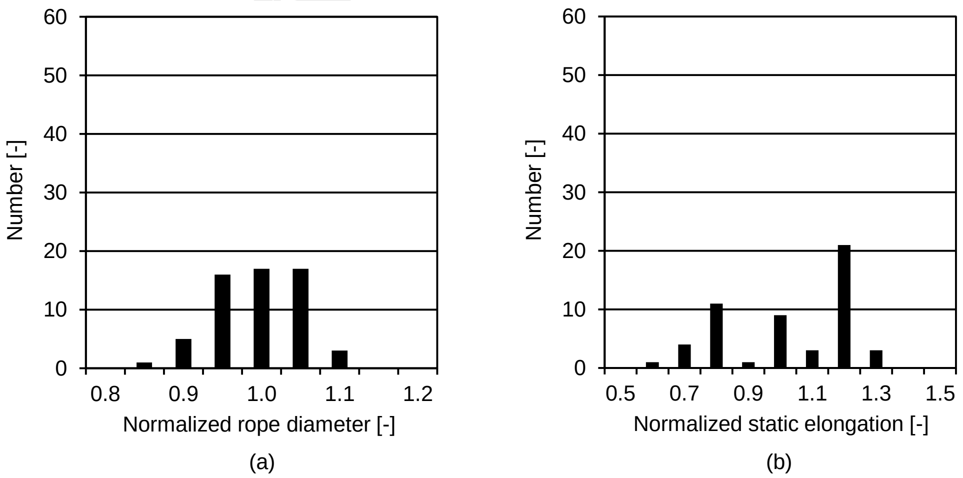

It can thus be concluded that static elongation and rope diameter are much less relevant in practice. The static elongation mainly comes into play in abseiling and ascending, where low values are desirable (which is why static ropes are often used in these cases). The rope diameter, meanwhile, is more relevant for durability, weight, and performance of the belay device. If it is too low, some devices will not work properly, making it vital to properly match rope and belay device. Table 7 summarises the results in respect of these desired rope properties.

Table 7. *Summary Rope Analysis*

		Desired rope properties			Sum-mary im-perative rope pro-perties
		High energy ab-sorption	Low max. accelera-tion	Low max. jerk	
Im-perative rope values	Peak force	Low	Low	Minor influence *)	**Low**
	Dynamic elonga-tion	High	Invariable	High	**High**
	Static elonga-tion	Minor influence	No influence	Minor influence	**Minor influence**

*) The influence of the peak force on the maximum jerk is minor with a high dynamic elongation.

Conclusion

The behaviour of dynamic single climbing ropes has been theoretically studied in an investigation covering 175 commercially available ropes from a wide range of manufacturers. For the first time, the effects of various rope parameters were systematically analysed, and different characteristic values (desired rope properties) identified by means of numerical simulation.

It was found that to minimise the risk of injury for a falling climber, it is necessary to have a high dynamic elongation. In terms of acute injury potential, a low peak force is less relevant, but it too must be kept low to minimise the load on all parts of the safety chain. Conversely the static elongation has only a minor influence.

Even though all studied ropes met the requirements of EN 892, some were clearly more desirable from a safety point of view than others. It was found that only about one third had the desired combination of low peak force and high dynamic elongation.

REFERENCES

Andrew, K. 2006. *An assessment of the effect of water absorption on the mechanical properties of dynamic climbing ropes* (Report 200231951). University of Strathclyde.

Beal, M. 2002. *Influence of parameters in the rope construction*. Proceedings of nylon and ropes for mountaineering and caving, Torino, Italy.

Bennett, F. 2000. *Learning the ropes*. Summit, 28-29.

Blackford, J.R. 2003. *Materials in mountaineering*. In M. Jenkins (Ed.), Materials in sports equipment (pp. 279-325). Woodhead: Abington Cambridge.

Burton, R., & Whinnery, J.E. 1985. *Operational G-induced loss of consciousness: something old; something new*. Aviation, Space, and Environmental Medicine, 812-817.

Crawford, H. 2003. *Survivable impact forces on human body constrained by full body harness* (Report). Health & Safety Executive HSE, UK.

EN 892:2012. 2012. *Mountaineering equipment – dynamic mountaineering ropes – safety requirements and test methods*.

European Directive 89/686/EEC. 2013. *Council directive of 21 December 1989 on the approximation of the laws of the Member States relating to personal protective equipment (PPE)*.

Karrer, R. 2002. *The perfect rope – production and use*. Proceedings of nylon and ropes for mountaineering and caving, Torino, Italy.

Lutz, M., & Mair, P. 2002. AnseilART - *Verletzungsmuster beim Sturz ins Seil* [Injury types caused by fall arrest devices]. bergundsteigen, 50-53.

Pavier, M. 1998. *Experimental and theoretical simulations of climbing falls*. Sports Engineering, 1, 79-91.

PPE Guidelines. 2010. *Guidelines on the application of council directive of 21 December 1989 on the approximation of the laws of the Member States relating to personal protective equipment*.

Reali, G., & Stefanini, L. 1996. An important question about rock climbing. European Journal of Physics, 17, 348-352.

Schambron, T., & Uggowitzer, P.J. 2009. *Effects of wear on static and dynamic failure loads of aluminium-based alloy climbing karabiners*. Sports Engineering, 11, 85-91.

Schubert, P. 2000. *About ageing of climbing ropes*. UIAA, p. 12-13.

Smith, R.A. 1998. *The development of equipment to reduce risk in rock climbing*. Sports Engineering, 1, 27-39.

Citation removed for review purposes.

UIAA. 2013. *Regulations for existing and potential UIAA accredited laboratories*. Version V_10.

UIAA 101-6.0. 2014. *Mountaineering and climbing equipment – dynamic ropes*.

Voshell, M. 2004. *High acceleration and the human body*. Retrieved from https://archive.4plebs.org/boards/tg/image/1412/80/1412809449468.pdf.

Weaver, C.S., & Sloan B.K., & Brizendine E.J., & Bock, H. 2006. *An analysis of maximum vehicle G forces and brain injury in motorsports crashes*. Medicine & Science in Sports & Exercise, 38, 246-249.

Rope manufacturers in alphabetical order:

Anpen. http://www.anpen.net/products_list/&pmcId=35.html.

Austrialpin. http://www.austrialpin.at/bergsteigen/ropes.aspx.

Beal. http://www.beal-planet.com/2014/anglais/cordes.html.

Blacksafe. http://www.blacksafe.de/de/seile.html.

Blue Water. https://bluewaterropes.com/product-category/ropes/.

CAMP. http://www.camp.it/IT/template03.aspx?codicemenu=868.

Consolidated Cordage. http://products.consolidatedcordage.com/viewitems/kernmantle-and-rescue-rope/dynamic-kernmantle-rope?&bc=100|1008|1084.

Cousin. http://fr.calameo.com/read/00322980477cfde5d774d.

CT. http://www.climbingtechnology.com/en-US/climbing/ropes-dynamic.html.

DMM. http://dmmclimbing.com/products/ropes-&-cord/.

Edelrid. http://www.edelrid.de/en/Edelrid/Sports/Ropes/.

Edelweiss. http://www.edelweiss-ropes.com/en/5-single-rope.

Gilmonte. http://www.gilmonte.eu/en-ropes-dynamic.php.

Kaya http://www.kayaropes.com/en/product-122-lupa_dynam%C4%B1c.

Mammut. http://www.mammut.ch/en/productOverview/products_ropes_single_ropes_ch/Single-Ropes.html.

Marlow. http://www.marlowropes.com/safety-and-access-products/ropes/dynamic-climbing-rope.html.

Metolius. http://www.metoliusclimbing.com/dynamic_ropes.html.

Millet. http://www.millet.fr/en/products/spring-summer-2015/hardware-ropes.

New England. http://www.teufelberger.com/en/products/climbing-recreation/maximr-dynamic-ropes.html.

Petzl. http://www.petzl.com/en/Sport/Ropes?l=US#.VR036bUcSHs.

PMI. http://dynamic.pmirope.com/products/.

Ridgegear. http://www.ridgegear.com/products/rga12r_dynamtr_dynaflex.php#.VTTHPrUcTTs.

Roca. http://techrock.es/index.php-mmod=staticContent&IDf=184.html.

Salewa. http://www.salewa.us/en/hardware/ropes-and-ropebags.html/?_ga=1.65637358.1327449866.1427978921.

Singing Rock. http://www.singingrock.com/ropes.

Skylotec. http://www.skylotec-sports.com/seile.

Sterling. http://www.sterlingrope.com/c/climbing_dynamic-ropes.

Tendon. http://www.mytendon.com/dynamic-ropes.

Trango. https://www.trango.com/s-5-climbing-ropes.aspx.